



Analyzing Single Peristaltic Wave Behavior in Ureter with Variable Diameters: A Ureterdynamic Study

Laxmikant G Keni¹, Satish Shenoy B¹, Chethan K N¹, Padmaraj Hegde², Prakashini K³, Masaaki Tamagawa⁴, Mohammad Zuber^{1,*}

¹ Department of Aeronautical & Automobile Engineering, Manipal Institute of Technology, Manipal Academy of Higher Education, Manipal-576104, India

² Department of Urology, Kasturba Medical College & Hospital, Manipal Academy of Higher Education, Manipal-576104, India

³ Department of Radio Diagnosis, Kasturba Medical College & Hospital, Manipal Academy of Higher Education, Manipal-576104, India

⁴ Department of Biological Functions and Engineering, Kyushu Institute of Technology, Japan

ARTICLE INFO

Article history:

Received 22 July 2023

Received in revised form 20 August 2023

Accepted 25 September 2023

Available online 1 January 2024

Keywords:

Variable diameter ureter; Peristaltic wave; CFD; Pressure; Velocity; Wall shear

ABSTRACT

Ureters are muscular tubes that transport urine from the kidney to the bladder. The peristalsis wave is responsible for carrying urine to the bladder. With the regular appearance of peristalsis, areas with anatomic narrowing junctions are crucial for ureteral diseases. A three-dimensional flow analysis is performed for different time steps to understand the effect of the urine bolus formation and the reflux phenomenon on variable diameter ureters. For the constant and variable diameter ureter, the pressure is obtained behind and in front of the propagating bolus respectively. The peristalsis wave creates the high-velocity of a jet in the neck region of the ureter. The contraction produces the trapping of the bolus leading to adverse flow in the contraction region. By virtue tapering, the high-pressure gradient builds up, leading to high wall shear in the ureter. The main goal is to determine the pressure, velocity, gradient pressure, and shear force on the ureter wall during peristaltic motion. These parameters are very important for clinicians to understand its effect in the unobstructed variable diameter ureter. This article may help to build a medical device for engineers. The physical significance of this information lies in its profound insights into the biomechanics and functionality of the ureters, which are essential components of the human urinary system.

1. Introduction

The ureter is a muscular tube with a length of approximately 25-30 cm long tube [1–3]. The pacemakers in the renal pelvis coordinate the rhythmic tightening and relaxing of the ureter muscles to form a peristalsis wave to transport the urine from the kidney to its temporary storage location in the bladder via the ureter [4, 5]. The rhythmic tightening and relaxing of the ureter muscles help urine bolus motion in the ureter. This process occurs about 1 to 8 times per second in the ureter with an average frequency of around 3 times per second, depending on various factors such as hydration

* Corresponding author.

E-mail address: mohammad.zuber@manipal.edu (Mohammad Zuber)

<https://doi.org/10.37934/cfdl.16.4.5468>

level, bladder pressure, and overall health of the individual [6, 7]. Due to anatomical conditions, the urine flow rate can affect the rhythmic tightening and relaxing of the ureter muscle [8, 9]. A normal urine flow rate for an adult human is generally around 20 mm/s to 60 mm/s [10, 11]. Researchers carry out many studies to understand the peristaltic behaviour and its biomechanics during the urine flow in the ureter [12–14] for theoretical and numerical analysis. Najafi *et al.*, [14] used two-dimensional and three-dimensional ureter models with the percentage of the block in the ureter to study the urine reflux and trapping phenomena in the ureter. They found that as the obstruction ratio increased, leads to an increase in the pressure gradient, reflux, and ureter wall shear stresses. Ureter mechanical properties are important for fluid-structure interaction [FSI] analysis [15–17]. In a recent study conducted by Takaddus *et al.*, [18, 19], the effects of flow on the ureter wall were investigated using both two-dimensional and three-dimensional circular tubes. To assess these effects, fluid-structure interaction (FSI) was utilized. The results of this study demonstrated that as obstruction increased, there was a corresponding increase in pressure gradient, shear stress, and reflux within the fluid. Vahidi *et al.*, [20] utilized the actual ureter model to investigate and analyze the flow dynamics occurring within the ureter. To conduct their analysis, they employed a two-dimensional Fluid-Structure Interaction (FSI) model. The results of their research demonstrated that urine reflux towards the kidney occurs due to wave onset in the ureter. As this wave travels towards the outlet, there is a noticeable decrease in reflux at the ureteropelvic junction. Li *et al.*, [21] used numerical modelling to analyze the peristalsis transport. They compared the result of the two-dimensional channel and the axisymmetric tube and found that the pressure gradient doesn't vary in the radial direction. Also, the inertia of the fluid and large wavelength produces the reflux near the axis of symmetry. In their research study, Vahidi *et al.*, [22] conducted an in-depth analysis of two-dimensional actual ureteral data using the non-linear fluid-structure interaction model. The researchers explored various aspects related to the flow of fluids and structures within the ureteral system. In a study conducted by Rassoli *et al.*, [23], the Mooney-Rivlin model was utilized to investigate and predict the behaviour of human ureters during peristalsis. They aimed to understand the mechanical response of the ureter and conducted a biaxial study for this purpose. Their findings revealed that the ureter wall behaves as an anisotropic material, which means it exhibits different mechanical properties in various directions. This finding helps to improve our understanding of force transmission through the ureteral walls during peristalsis, ultimately leading to better treatment options for related medical conditions. Moreover, they also discovered that hyperplastic modeling could be used to accurately represent the behavior of human ureters. Hosseini *et al.*, [24] reviewed the experimental, theoretical, and numerical studies on the ureter. They considered the mechanical properties of ureters to develop the virtual simulation tool to present the contraction of the ureter by pacemaker activities. In the field of urology, extensive research has been conducted on various aspects related to the ureter. However, it is important to note that most of this research has focused on a specific type of ureter - the constant diameter ureter. Researchers have explored different aspects such as anatomy, physiology, pathology, and clinical management pertaining specifically to the constant diameter ureter. In a recent study conducted by Srivastava *et al.*, [25–27], the effects of fluid viscosity variation on peristaltic transport in non-uniform tubes and channels were investigated. The researchers considered various factors such as inlet and outlet radius, wave speed, and fluid velocity to determine the pressure changes during peristalsis. Specifically, they set the inlet and outlet radii at 0.012 cm and 0.018 cm respectively while assuming that the peristalsis wave travels along a 20 cm long wall at a speed of 20 cm/s. The results of their analysis showed that pressure decreases with decreasing viscosity but increases with increasing flow rate. Additionally, it was observed that fluid velocity decreased as a result of these changes in pressure. Misra *et al.*, [28] conducted a comprehensive study on the peristaltic flow in an axisymmetric variable cross-section

circular pipe. Their research focused on analyzing the Reynolds and wave numbers under lower conditions based on second-order assumptions. The researchers considered various parameters such as tapered length, velocity of the wave, and radius to investigate their effects on the peristalsis flow [29, 30]. The study involved examining pipes with radii ranging from 0.01cm to 4 cm over a distance of 20 cm. They found that increasing the velocity led to an increase in amplitude ratio, indicating that higher velocities result in stronger waves propagating through the pipe. They also found that there was no significant change observed in either Reynolds number or velocity when wave number is varied. Eytan *et al.*, [31] conducted a comprehensive study on the peristalsis flow in the uterus. The researchers analyzed the effect of the flow field due to sinusoidal phase shift and angular effect on the tapered wall of the uterus. They used advanced computational models to simulate different scenarios and investigated the changes in these parameters that affect various aspects of peristalsis. They discovered that when contractions are out of phase, there is a significant reduction in velocity, pressure, and flow rates within the uterus. This suggests that proper coordination between different regions of the uterus is necessary for efficient peristaltic movement. Moreover, they also observed that as the angle of tapering increases, there is an increase in the reflux phenomenon - this means that more fluid flows back into previous sections instead of moving forward toward its destination. On the other hand, with smaller angles comes increased trapping which can lead to complications such as blockages or infections. In recent years, researchers [25–28, 31] have been investigating the peristalsis activity on a tapered ureter to gain a better understanding of its functions. This has led to significant advancements in computational techniques [32–34] and finite element analysis that are now widely used in medical applications. In this particular study, an unobstructed three-dimensional finite variable diameter ureter was analyzed to investigate the peristaltic effect [35]. The results of this study can provide clinicians with a comprehensive introduction to understanding the human ureter during peristalsis. By analyzing pressure, velocity, and wall shear effect during peristalsis, researchers were able to gain insight into these factors affect the function of the ureter. This information is crucial for developing effective treatments for conditions that affect the urinary system. Overall, this study highlights the importance of using advanced computational techniques and finite element analysis in medical research [36, 37]. In total, the novelty of this content lies in its comprehensive and multidimensional approach to studying the variable diameter ureter, incorporating advanced computational techniques, fluid viscosity variation, and the broader implications of peristalsis research. This approach enhances our understanding of the urinary system and its clinical applications, marking a significant contribution to the field of medical research.

2. Methodology

2.1 Modeling and Meshing

There were certain areas with anatomic narrowing play a crucial role in ureteral disease. These areas include the ureteropelvic junction, where the renal pelvis connects to the ureter; the ureterovesical junction, where the ureter meets with the bladder; and finally, iliac vascular junctions located near major blood vessels in our pelvic region. The importance of these narrow points lies in their susceptibility to blockages or other issues that can cause problems for urine flow through these critical pathways [38]. Urogram studies have cited different numbers of diameter sizes in transverse sections, which can vary depending on the specific sample population being studied. For example, a study focused on post-partum females may derive slightly different size ranges than a study focused on males or non-postpartum females. In general, these sizes range from 2 mm to 8 mm [39–41], indicating that there is some variability in the size of structures within the urinary tract across individuals and populations. The total length of the ureter varies between individuals, but on average

it ranges from 220 mm to 300 mm [42–44]. To better understand the anatomy of this vital structure, we can divide its length into three parts: upper, middle, and lower. The upper part starts at the pelvis and extends up until it reaches the UPJ (ureteropelvic junction). From there, we have the upper ureter 1/3 which goes from UPJ until reaching the upper edge of the sacrum; then comes the middle ureter 1/3 which extends from the upper edge down to the lower edge of the sacrum; finally, we have the lower ureter 1/3 that stretches all way down from the lower edge of sacrum until reaching bladder. Additionally, segmental anatomy lengths can range anywhere between 74 mm to 100 mm [41].

In the current investigation, a length of 100mm is considered for the ureter with variable diameter, as illustrated in Figure 1. We modelled a three-dimensional ureter using Ansys 2019-R2. For the modelling of the ureter, an inlet diameter of 3 mm and an outlet diameter of 2 mm is considered. Due to peristalsis, a maximum diameter of 4 mm can be assumed for our current model. This means that as fluid flows through the ureter, its shape changes due to these muscular contractions. The analysis was performed using the commercially available package Ansys-CFX for computational dynamics.

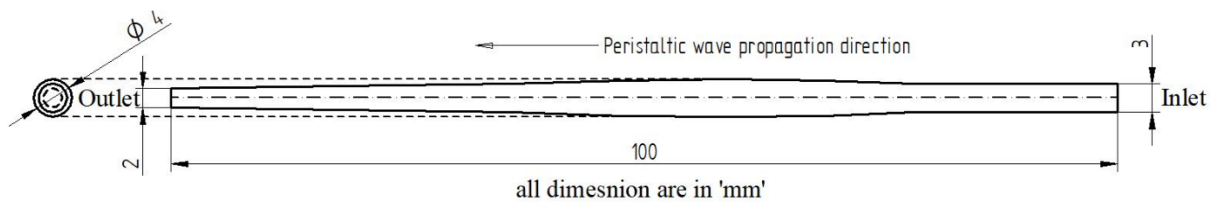


Fig. 1. Variable diameter ureter geometry

For the pressure and momentum calculation, a second-order upwind scheme is adopted [20]. Figure 2 shows the meshed model of the tapered ureter. Diffusion-based smoothing is used for the mesh motion. To conduct a thorough analysis, a total wave cycle of 9 s is simulated. This setting helps to gather enough data and observe any patterns or trends that may occur over time. To ensure output accuracy, the time interval is set at 0.05 s.

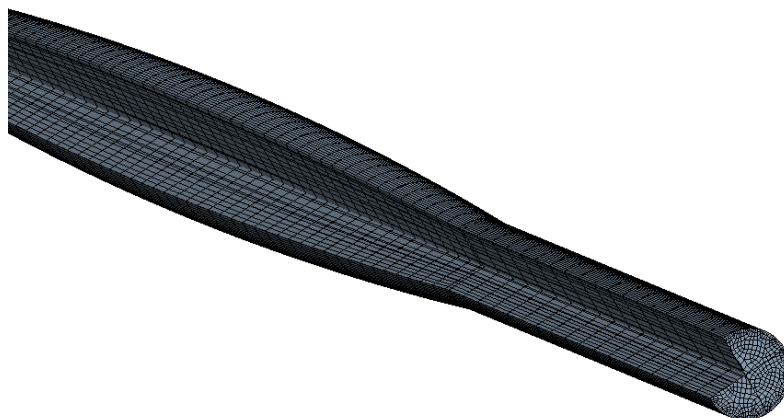


Fig. 2. The cross-sectional view of a meshed structure of the variable diameter ureter

2.2 Mesh Grid Independence Study

Before carrying out different sets of analyses, we performed a grid independent analysis to finalize the optimum mesh size. In this work, structured mesh techniques are used [44]. To determine

the consistent results the mesh grid size is varied from 0.05 mm to 0.008 mm. Our findings are presented in Figure 3, which shows the mesh grid independence results. It is observed that there is a significant increase in the pressure values when the mesh size is reduced from 0.05 mm to 0.01 mm. However, when the mesh size was reduced further than 0.01 mm the pressure difference was observed to be less than 5%. So to avoid the higher computational time with an optimized mesh value, a mesh size of 0.01 mm is used in all the analyses performed in this work. A finite element model was created using a mesh size of 0.01 mm, resulting in 69,552 nodes and 79,091 elements.

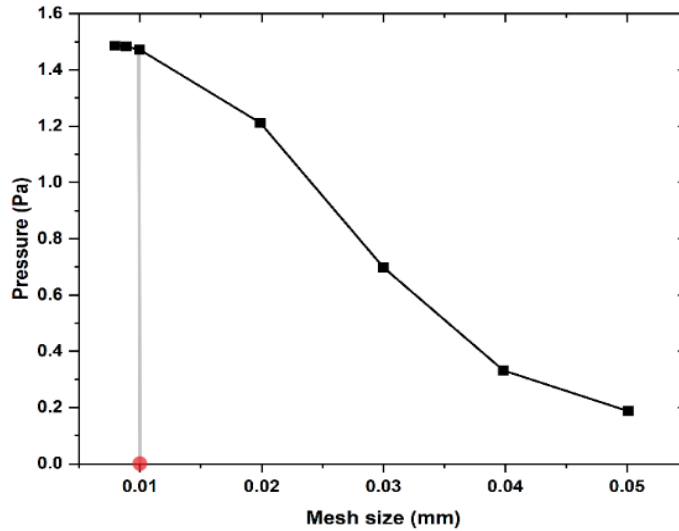


Fig. 3. Mesh grid independence with variation in pressure

2.3 The Governing Equation

For the analysis, urine is often considered to be a homogenous liquid, additionally, it is characterized as being viscous, which refers to its resistance to flow. To further understand the behaviour of urine during flow, the Navier-Stokes equation was adopted. This equation takes into account several factors that can affect fluid dynamics including density and viscosity. For this particular study, a density (ρ) of 1050 kg/m³ and a viscosity (μ) of 1.3 cP [45] were chosen for use in the Navier-Stokes equation.

For the flow model, the governing equation given by,

The continuity equation is,

$$\nabla \cdot \mathbf{u}_f = 0 \quad (1)$$

The momentum equation is,

$$\frac{\partial \mathbf{u}_f}{\partial t} + (\mathbf{u}_f \cdot \nabla) \mathbf{u}_f = -\nabla p + \frac{\mu}{\rho} (\nabla^2 \mathbf{u}_f) \quad (2)$$

The velocity vector is denoted by \mathbf{u}_f , while p represents pressure, ρ stands for density, and μ denotes fluid dynamic viscosity. To solve equations that involve these variables, several methods have been proposed over the years. One such method is known as the Semi-Implicit Method for

Pressure Linked Equations (SIMPLE). This method involves an iterative approach to obtain a solution for discretized equations. The SIMPLE method has proven to be quite effective in solving problems related to fluid dynamics. The iterative nature of this method allows it to handle complex systems with ease and efficiency [46].

2.4 Peristaltic Motion

During peristalsis, which is a series of coordinated muscle contractions, the velocity range in the ureter can vary from 20 to 60 mm/s [47]. In current research work, a peristaltic wave with a velocity of 20 mm/s can be applied in a sinusoidal form to these walls.

Equation 3 is adopted to measure the displacement that occurs in the ureter wall during this process. In this particular scenario, three important parameters describe the characteristics of a wave. The first parameter is the amplitude of displacement (a), which has a value of 1 mm. The second parameter is known as wave number (k) and it has a value of 2. Wave number represents the number of waves that exist per unit length in space. Finally, the frequency (ω) with a value of 1 Hz.

$$d(z, t) = \pm a \sin(kz) \sin(\omega t) \quad (3)$$

3. Result and Discussion

To study the dynamics of ureters, a three-dimensional model was created. The simulation was conducted over a total wave cycle of 9 s, during which a wave velocity of 20 mm/s propagated from the inlet to the outlet. To gain further insights into this process, various parameters were analyzed in detail between time intervals of 1 s to 8 s. These included pressure, velocity, and wall shear stress.

3.1 Pressure Contour Analysis

In this study, a variable-diameter ureter model was used to investigate the flow of urine through the ureter. To simulate physiological conditions, a peristaltic wave was applied to the ureteral wall from the inlet to the outlet. A constant pressure difference of 0.3 Pa boundary condition was imposed at both ends of the model to create a realistic scenario. The results of this simulation are presented in Fig 4, which shows pressure profile contours for different time points during the flow process. At $t=2$ s, when urine starts flowing into the ureter due to peristalsis, we can observe changes in pressure distribution along its length. The variable diameter ureter indicates the convergence flow condition of the fluid dynamics study. It was observed that at the time of 3 s, the bolus entered the ureter, and the maximum pressure was obtained in the front of the neck, as shown in Figure 4 (a), due to the convergence in the area and the formation of the neck due to the peristalsis. During wave propagation to the outlet, the pressure experienced by urine decreases. This phenomenon is depicted in Figure 4 (b), which shows a decrease in pressure as waves propagate toward the outlet. The maximum pressure developed behind the propagating urine bolus was reported by Weinberg [48] for the constant-diameter ureter. However, our investigation of variable diameter ureters has revealed that there are some differences when it comes to where maximum pressure is created during wave propagation. In contrast to Weinberg's [48] findings, we have discovered that in variable diameter ureters, maximum pressure is created in front of the propagating bolus rather than behind it.

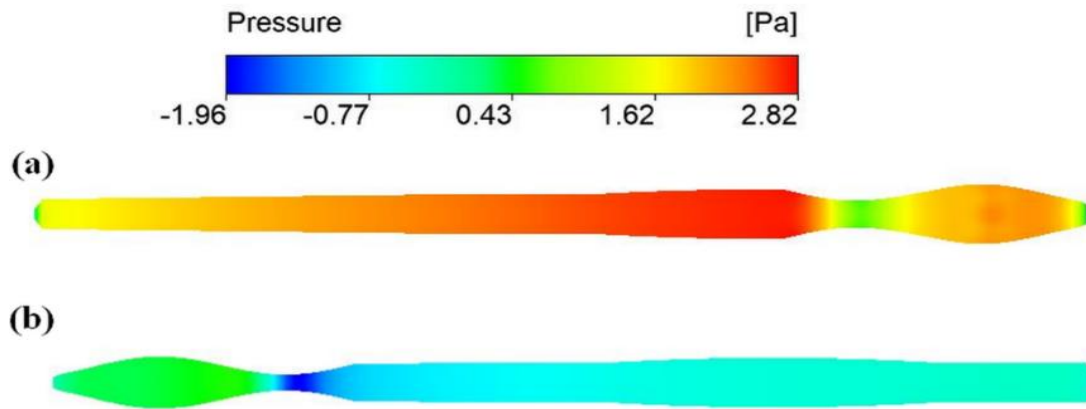


Fig. 4. Pressure contours (a) peristalsis wave at time 3 s (b) peristalsis wave at time 7 s

In the research study, Figure 5 is presented to depict the pressure plots along the ureter length for a specific time interval ranging from 3 s to 8 s. The data obtained from this analysis provides us with valuable insights into the effects of pressure on the ureter. As per the findings, it was observed that at 3 s, there was a significant increase in maximum pressure of up to 1.56 Pa due to two key factors - tapered area and reduction in the area caused by peristalsis. This narrowing creates resistance against fluid flow and leads to an increase in pressure within that region. Takaddus *et al.*, [18] found that at UPJ, maximum pressure develops due to peristalsis contraction. In the present work, the maximum pressure of 1.56 Pa develops at the inlet of the ureter, that is at UPJ. As the wave travels to the outlet due to a reduction in the area, the pressure decreases at the outlet of the variable diameter ureter.

It has been observed that for the ureter with constant diameter, there is a decrease in pressure distribution along its axis towards the exit as noted by Eytan *et al.*, [31] and Vahidi *et al.*, [20] in their studies. However, recent research findings have revealed that when waves travel through variable ureters, such as those with narrowing regions, there is also a significant decrease in pressure toward the outlet as in Figure 4(b). This implies that variations in diameter along the length of ureters can significantly affect their functionality and may cause complications if not addressed promptly.

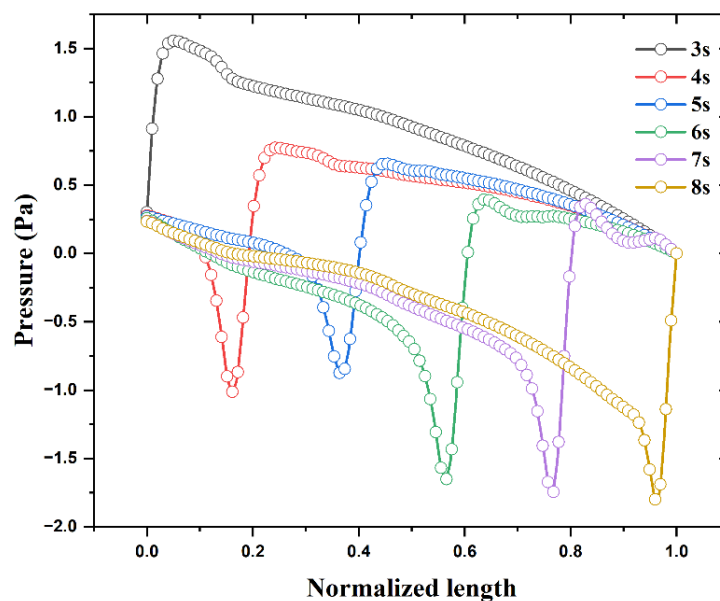


Fig. 5. Pressure profile plot for variable diameter ureter

The process of peristalsis in the ureter involves the formation of a bolus and neck during wave propagation. According to Weinberg's [48] research, a single peristaltic wave on a constant diameter ureter generates pressure behind the propagating wave. However, when it comes to variable diameter ureters, pressure is observed to generate in front of the bolus. In Figure 6, we can see that negative pressure forms due to peristalsis in the neck region leading to reflux formation in the ureter after 3 s of flow time. This observation is consistent with Vahidi *et al.*, [49] findings for constant diameter ureters where reflux occurs at the onset of wave propagation at the kidney and decreases as it moves towards an outlet. Interestingly, our study on variable diameter ureters found that maximum pressure without any reflux occurred at the beginning of wave propagation show in Figure 6. As expected, there was a reduction in pressure as waves propagated further along similar lines with Vahidi *et al.*, [49] observations for constant-diameter ureters.

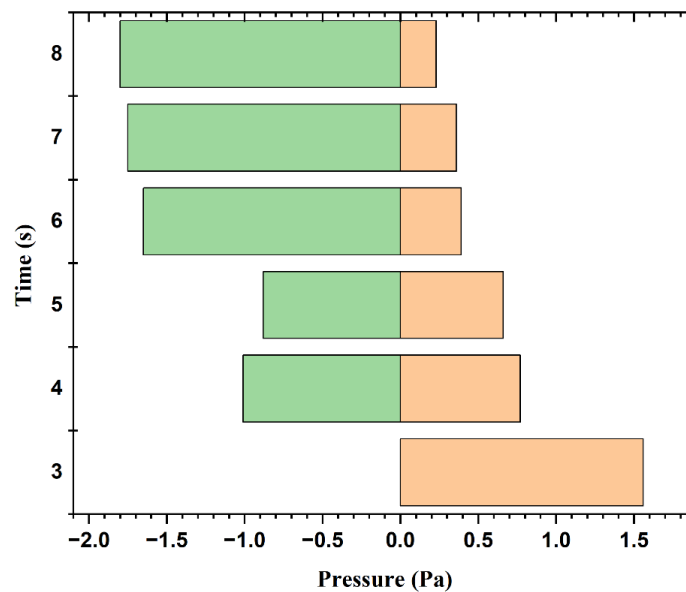


Fig. 6. Pressure plot at flow time steps

3.2 Velocity Profile Analysis

Figure 7 displays the velocity vector plot for the variable diameter ureter at the onset of wave propagation. At time 3 s, peristalsis initiates and a reverse flow is detected at the inlet as illustrated in Figure 7(a). As this wave progresses, it leads to the formation of a jet with high velocity in the neck region due to the narrowing and contraction of the ureter area. This phenomenon can be observed in Figure 7(b), Hosseini *et al.*, [50] also reported similar findings that maximum flow occurs at contracted regions due to fluid inertia. The peristaltic movement causes contractions that trap boluses because of reverse flows occurring in the neck region.

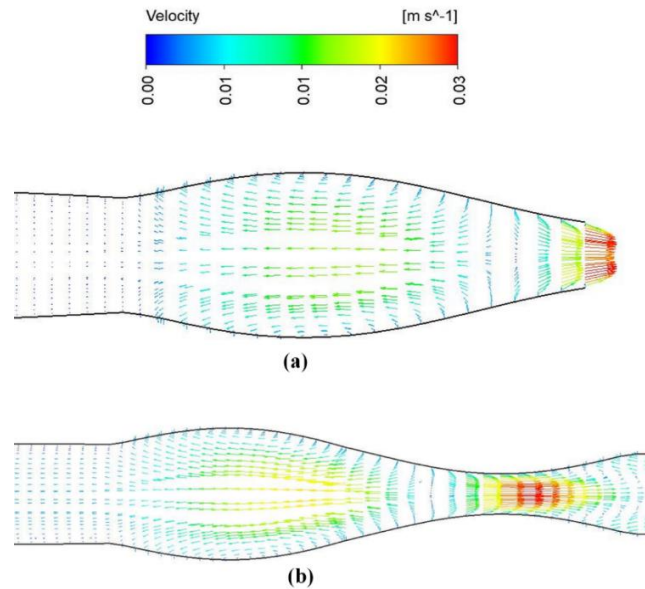


Fig. 7. Variable diameter ureter Velocity vector for (a) peristalsis wave at 3 s (b) peristalsis wave at 3.5 s

Figure 8 shows the velocity profile plot for the variable diameter ureter. The neck region recorded the magnitude of a velocity of 0.0411 m/s at time 4 s. As the wave propagates further at time 5 s, velocity decreases. As the wave crosses the median length of the ureter at time steps 6 s and 7 s, due to a reduction in the area along the length, the rise in velocity was again recorded. It is clear from the graph shown in Figure 8 that the contraction produces the jet of flow in the ureter, which results in a high-velocity magnitude in the plot.

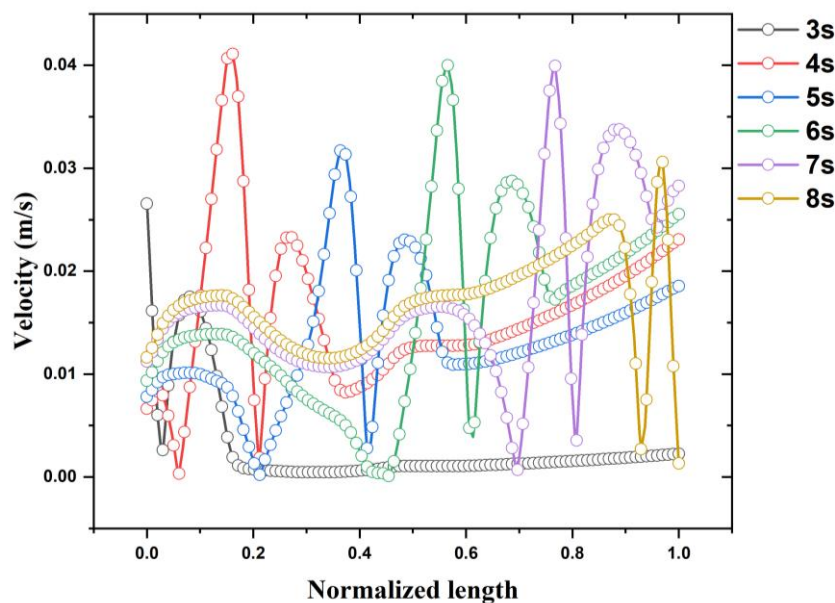


Fig. 8. Velocity profile plot for variable diameter ureter

Figure 9, describes the maximum and minimum velocity generated during the peristalsis motion for different flow time steps. The graph provides a clear insight into the flow dynamics of urine through the ureter. As per the graph, it is evident that the highest magnitude of velocity is developed at 4 s when urine enters the ureter. This sudden surge in velocity could be attributed to various

factors such as the contraction of smooth muscles surrounding ureters or pressure changes caused by urinary bladder contractions. Furthermore, we notice two more peaks in velocity at 6 s and 7 s on the graph. These peaks are due to a reduction in geometrical area and neck formation caused by peristalsis waves travelling down towards its outlet. As these waves travel further downstream towards their outlet, they tend to dissipate gradually resulting in reverse flow disappearing near the inlet of the ureter.

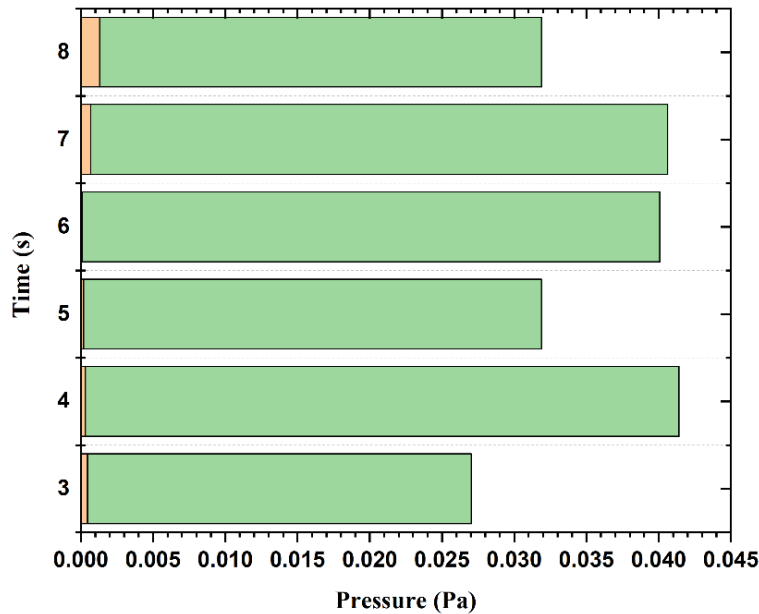


Fig. 9. Velocity plot at flow time steps

3.3 The Pressure Gradient Analysis

The pressure gradient is an important factor to consider in the study of ureter dynamics. The results of this analysis are presented in Figure 10, which shows the pressure gradient along the axis for different time steps. It was observed that the maximum pressure gradient occurs during the contraction produced by the peristaltic wave. Furthermore, it can be seen from Figure 10 that there are peaks in the plot corresponding to the high and low-pressure formation during wave propagation on the ureter wall. These peaks represent changes in pressure as a result of variations in cross-sectional area along the length of the ureter. Finally, it should be noted that our analysis revealed a maximum pressure gradient of 607.7 Pa/m recorded during the contraction of the ureter wall at a time step of 7 s. This contraction is observed on the ureter at the outlet. This contraction can be seen clearly in Figure 10. Interestingly, it has been found that pressure gradients do not significantly affect the renal pelvic region (inlet) of a variable diameter ureter. However, as a wave travels through the ureter, it generates maximum pressure near its outlet which can potentially cause damage to the urethral wall at their junction. Understanding such processes is crucial for developing effective treatments for urinary tract disorders and improving overall health outcomes.

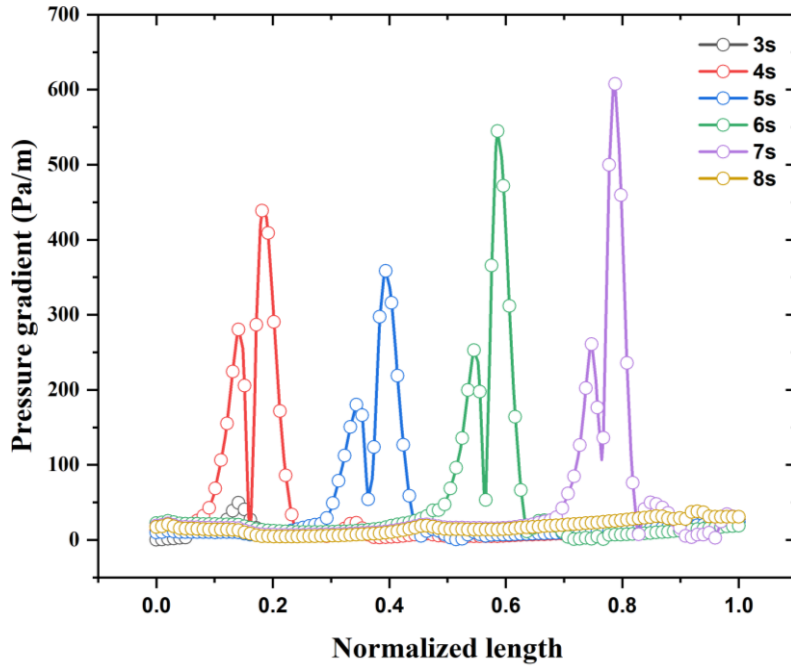


Fig. 10. Pressure gradient plot for the variable ureter diameter

3.4 The Wall Shear Stress Analysis

Figure 11 shows the wall shear stress developed during the bolus motion from the inlet to an outlet for the variable diameter ureter. It was found that the maximum shear magnitude of 0.111 Pa is located near the outlet at the time of 7 s. The high values recorded in the plot were due to contraction at these time intervals from 3 s to 8 s. Hosseini *et al.*, [42], and Vahidi *et al.*, [41] found that high shear stresses arise in the area around the contraction. It is clear from Figure 10 and Figure 11 that the maximum pressure gradient leads to maximum wall shear.

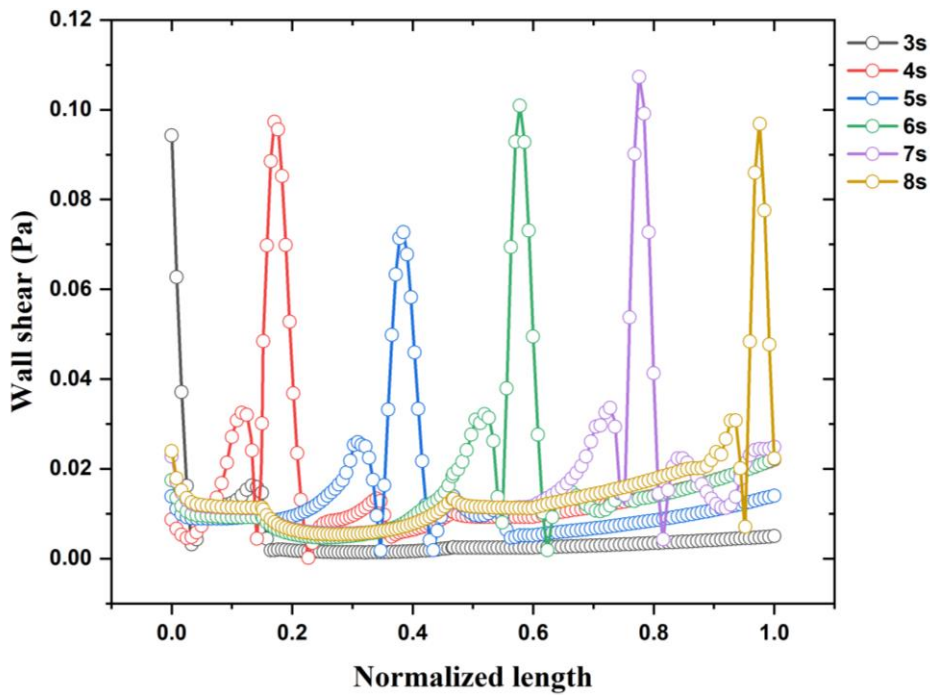


Fig. 11. Wall shear plot for variable diameter ureter

3.5 Limitations of the Current Work

The study used variable diameter ureters to explore pressure dynamics. Results showed high-pressure regions in front of the bolus, but pressure decreased towards an outlet. Reflux occurred in the neck region. Ureter diameters vary from 2 mm to 8 mm despite being commonly considered 3mm or 2 mm. It has been observed that multiple peristaltic waves can be simulated on the variable diameter ureter and length. However, it is important to note that a fixed input velocity of 20 mm/s was considered for this study. It would be interesting to explore different input velocities could affect the peristaltic effect on the ureter wall. This could provide us with a better understanding of changes in flow rate or speed may impact urinary tract function. To further investigate this phenomenon, rapid prototype techniques have been suggested as an effective means of creating a 3D-printed model of the ureter for experimental analysis. By using such models, researchers can simulate various conditions and observe the peristalsis in real time.

4. Conclusion

The study examined the ureter's diameter during peristaltic wave motion and found it has three segments with varying lengths of 74-100 mm. A standard length of 100mm was used for consistency in measurements. At time step 2 s, the urine starts flowing into the ureter. The first bolus formation commences at a time step of 3 s and ends at 8 s. Hence the ureter wall is analyzed at 3 s to 8 s, it was found that the maximum pressure is generated in front of the propagating bolus. However, the maximum pressure is found behind the bolus in the constant diameter ureter. For the peristaltic wave motion, the maximum pressure of 1.56 Pa is recorded at 3 s due to the reduction in the area at the inlet of the ureter. Due to a narrowing in the area towards the outlet, the pressure will decrease. It was found that in the neck region, the negative pressure formed due to peristaltic, leading to reflux formation in the ureter. Contraction and the narrowing area result in a high-velocity jet flow in the neck region. The maximum velocity of 0.0411 m/s is recorded at time 4s. Trapping of a bolus by contraction in the flow leads to reverse flow formation in the neck region. The reverse flow advances the urinary tract infection and results in the bacteria and toxins from the UPJ to the kidney. This may further lead to serious kidney problems over a period of time. It was found that with a variable diameter ureter, the maximum pressure gradient is recorded at the contraction produced by the peristaltic wave. This contraction is observed on the ureter at the inlet. The maximum pressure gradient of 607.7 Pa/m and the maximum shear magnitude of 0.111 Pa are recorded at the wall contraction of the ureter in the time step of 7 s. The high shear stress can rupture the junctions in the ureter. This work has a clear idea for pressure and velocity plots for variable diameter, which mimics the flow generated by the patient-specific model. However, the rupture shear stress values are still unknown due to the properties of the ureter wall and the ureter density in each layer varying. These parameters are essential for clinicians to understand its effect in the unobstructed variable diameter ureter. This article may help to build medical devices for engineers. Further experimental work can be carried out by manufacturing ureter tubes using appropriate rapid prototyping techniques that help to understand the impact of shear stresses on constrictions of the ureter. Also, patient-specific modelling and analysis can be carried out to know the effect of the different wall densities of the ureter.

Acknowledgements

The authors would like to thank the Department of Aeronautical and Automobile Engineering, Manipal Institute of Technology, Manipal Academy of Higher Education, Manipal for the computing resources provided to carry out this research work.

References

- [1] Venkatesh D, Sudhakar HH. Textbook of Medical Physiology. Wolters kluwer india Pvt Ltd; 2018.
- [2] Hall JE, Guyton AC. Guyton and Hall Textbook of Medical Physiology. Saunders/Elsevier; 2011.
- [3] Mahadevan V. Anatomy of the lower urinary tract. *Surg* 2016;34:318–25. <https://doi.org/10.1016/j.mpsur.2016.04.001>
- [4] Feeney, Meghan M., and Norman D. Rosenblum. "Urinary tract pacemaker cells: current knowledge and insights from nonrenal pacemaker cells provide a basis for future discovery." *Pediatric nephrology* 29 (2014): 629-635. <https://doi.org/10.1007/s00467-013-2631-4>
- [5] Hammad, F. T. "Electrical propagation in the renal pelvis, ureter and bladder." *Acta Physiologica* 213, no. 2 (2015): 371-383. <https://doi.org/10.1111/apha.12392>
- [6] Weinberg, S. L., M. Y. Jaffrin, and A. H. Shapiro. "Hydrodynamic model of ureteral function." In *Urodynamics*, pp. 217-231. Academic Press, 1971. <https://doi.org/10.1016/B978-0-12-121250-6.50024-1>
- [7] Weinberg, Sidney R., and Thomas J. Maletta. "Measurement of peristalsis of the ureter and its relation to drugs." *Jama* 175, no. 1 (1961): 15-18. <https://doi.org/10.1001/jama.1961.03040010017005>
- [8] ATSUO, KONDO. "The Contraction of The Ureter: I. Observations in Normal Human and Dog Ureters." *Nagoya journal of medical science* 32, no. 3-4 (1970): 387-394.
- [9] Krstić, Radivoj V. *Human microscopic anatomy: an atlas for students of medicine and biology*. Springer Science & Business Media, 1991.
- [10] Griffiths, Derek J. "Dynamics of the upper urinary tract: I. Peristaltic flow through a distensible tube of limited length." *Physics in Medicine & Biology* 32, no. 7 (1987): 813. <https://doi.org/10.1088/0031-9155/32/7/002>
- [11] Griffiths, D. J., C. E. Constantinou, J. Mortensen, and J. C. Djurhuus. "Dynamics of the upper urinary tract: II. The effect of variations of peristaltic frequency and bladder pressure on pyeloureteral pressure/flow relations." *Physics in Medicine & Biology* 32, no. 7 (1987): 823. <https://doi.org/10.1088/0031-9155/32/7/003>
- [12] Gómez-Blanco, J. Carlos, F. Javier Martínez-Reina, Domingo Cruz, J. Blas Pagador, Francisco M. Sánchez-Margallo, and Federico Soria. "Fluid structural analysis of urine flow in a stented ureter." *Computational and mathematical methods in medicine* 2016 (2016). <https://doi.org/10.1155/2016/5710798>
- [13] Zheng, Shaokai, Dario Carugo, Ali Mosayyebi, Ben Turney, Fiona Burkhard, Dirk Lange, Dominik Obrist, Sarah Waters, and Francesco Clavica. "Fluid mechanical modeling of the upper urinary tract." *WIREs Mechanisms of Disease* 13, no. 6 (2021): e1523. <https://doi.org/10.1002/wsbm.1523>
- [14] Najafi, Z., B. F. Schwartz, A. J. Chandy, and A. M. Mahajan. "A two-dimensional numerical study of peristaltic contractions in obstructed ureter flows." *Computer Methods in Biomechanics and Biomedical Engineering* 21, no. 1 (2018): 22-32. <https://doi.org/10.1080/10255842.2017.1415333>
- [15] Knudsen, L., H. Gregersen, B. Eika, and J. Frøkiær. "Elastic wall properties and collagen content in the ureter: an experimental study in pigs." *Neurourology and urodynamics* 13, no. 5 (1994): 597-606. <https://doi.org/10.1002/nau.1930130515>
- [16] Sokolis, Dimitrios P. "Multiaxial mechanical behaviour of the passive ureteral wall: experimental study and mathematical characterisation." *Computer Methods in Biomechanics and Biomedical Engineering* 15, no. 11 (2012): 1145-1156. <https://doi.org/10.1080/10255842.2011.581237>
- [17] Najafi, Zahra, Prashanta Gautam, Bradley F. Schwartz, Abhilash J. Chandy, and Ajay M. Mahajan. "Three-dimensional numerical simulations of peristaltic contractions in obstructed ureter flows." *Journal of Biomechanical Engineering* 138, no. 10 (2016): 101002. <https://doi.org/10.1115/1.4034307>
- [18] Takaddus, Ahmed Tasnub, Prashanta Gautam, and Abhilash J. Chandy. "Numerical simulations of peristalsis in unobstructed human ureters." In *ASME International Mechanical Engineering Congress and Exposition*, vol. 50534, p. V003T04A024. American Society of Mechanical Engineers, 2016. <https://doi.org/10.1115/IMECE2016-65999>
- [19] Takaddus, Ahmed Tasnub, Prashanta Gautam, and Abhilash J. Chandy. "A fluid-structure interaction (FSI)-based numerical investigation of peristalsis in an obstructed human ureter." *International Journal for Numerical Methods in Biomedical Engineering* 34, no. 9 (2018): e3104. <https://doi.org/10.1002/cnm.3104>
- [20] Vahidi, Bahman, and Nasser Fatourae. "A biomechanical simulation of ureteral flow during peristalsis using intraluminal morphometric data." *Journal of theoretical biology* 298 (2012): 42-50. <https://doi.org/10.1016/j.jtbi.2011.12.019>
- [21] Li, Chin-Hsiu. "Peristaltic transport in circular cylindrical tubes." *Journal of biomechanics* 3, no. 5 (1970): 513-523.

- [https://doi.org/10.1016/0021-9290\(70\)90060-6](https://doi.org/10.1016/0021-9290(70)90060-6)
- [22] Vahidi, Bahman, and Nasser Fatourae. "Mathematical modeling of the ureteral peristaltic flow with fluid structure interaction." *measurements* 5, no. 6 (2007). <https://doi.org/10.1115/SBC2007-175513>
- [23] Rassoli, Aisa, Mohammad Shafigh, Amirsaeed Seddighi, Afsoun Seddighi, Hamidreza Daneshparvar, and Nasser Fatourae. "Biaxial mechanical properties of human ureter under tension." *Urology journal* 11, no. 3 (2014).
- [24] Hosseini, Ghazaleh, John JR Williams, Eldad J. Avital, A. Munjiza, Xu Dong, and James SA Green. "Simulation of the upper urinary system." *Critical Reviews™ in Biomedical Engineering* 41, no. 3 (2013). <https://doi.org/10.1615/CritRevBiomedEng.2013009704>
- [25] Srivastava, L. M., V. P. Srivastava, and S. N. Sinha. "Peristaltic transport of a physiological fluid." *Biorheology* 20, no. 2 (1983): 153-166. <https://doi.org/10.3233/BIR-1983-20205>
- [26] Srivastava, L. M., and V. P. Srivastava. "Peristaltic transport of blood: Casson model—II." *Journal of Biomechanics* 17, no. 11 (1984): 821-829. [https://doi.org/10.1016/0021-9290\(84\)90140-4](https://doi.org/10.1016/0021-9290(84)90140-4)
- [27] Srivastava, L. M., V. P. Srivastava, and S. N. Sinha. "Peristaltic transport of a physiological fluid. Part-III. applications." *Biorheology* 20, no. 2 (1983): 179-185. <https://doi.org/10.3233/BIR-1983-20207>
- [28] Misra, J. C., and S. K. Pandey. "Peristaltic transport in a tapered tube." *Mathematical and computer modelling* 22, no. 8 (1995): 137-151. [https://doi.org/10.1016/0895-7177\(95\)00162-U](https://doi.org/10.1016/0895-7177(95)00162-U)
- [29] Balachandra, H., Choudhari Rajashekhar, Hanumesh Vaidya, Fateh Mebarek Oudina, Gudekote Manjunatha, and Kerehalli Vinayaka Prasad. "Homogeneous and heterogeneous reactions on the peristalsis of bingham fluid with variable fluid properties through a porous channel." *Journal of Advanced Research in Fluid Mechanics and Thermal Sciences* 88, no. 3 (2021): 1-19.
- [30] Hadimani, Balachandra, Rajashekhar Choudhari, Prathiksha Sanil, Hanumesh Vaidya, Manjunatha Gudekote, Kerehalli Vinayaka Prasad, and Jyoti Shetty. "The Influence of Variable Fluid Properties on Peristaltic Transport of Eyring Powell Fluid Flowing Through an Inclined Uniform Channel." *Journal of Advanced Research in Fluid Mechanics and Thermal Sciences* 102, no. 2 (2023): 166-185. <https://doi.org/10.37934/arfmts.102.2.166185>
- [31] Eytan, Osnat, Ariel J. Jaffa, and David Elad. "Peristaltic flow in a tapered channel: application to embryo transport within the uterine cavity." *Medical engineering & physics* 23, no. 7 (2001): 475-484.
- [32] Nadeem, Sohail, Salman Akhtar, Anber Saleem, Nevzat Akkurt, Hassan Ali Ghazwani, and Sayed M. Eldin. "Numerical computations of blood flow through stenosed arteries via CFD tool OpenFOAM." *Alexandria Engineering Journal* 69 (2023): 613-637. <https://doi.org/10.1016/j.aej.2023.02.005>
- [33] Akhtar, Salman, Zahir Hussain, Zareen A. Khan, Sohail Nadeem, and Jehad Alzabut. "Endoscopic balloon dilation of a stenosed artery stenting via CFD tool open-foam: Physiology of angioplasty and stent placement." *Chinese Journal of Physics* 85 (2023): 143-167. <https://doi.org/10.1016/j.cjph.2023.06.018>
- [34] Akhtar, Salman, Zahir Hussain, Sohail Nadeem, IM R. Najjar, and A. M. Sadoun. "CFD analysis on blood flow inside a symmetric stenosed artery: Physiology of a coronary artery disease." *Science Progress* 106, no. 2 (2023): 00368504231180092. <https://doi.org/10.1177/00368504231180092>
- [35] Akhtar, Salman, Muhammad Hasnain Shahzad, Sohail Nadeem, Aziz Ullah Awan, Shahah Almutairi, Hassan Ali Ghazwani, and Mohamed Mahmoud Sayed. "Analytical solutions of PDEs by unique polynomials for peristaltic flow of heated Rabinowitsch fluid through an elliptic duct." *Scientific Reports* 12, no. 1 (2022): 12943. <https://doi.org/10.1038/s41598-022-17044-y>
- [36] Nadeem, Sohail, Shahah Almutairi, and Salman Akhtar. "A significant wave form analysis on the peristaltic flow in a duct with convection and diffusion effects." *Waves in Random and Complex Media* (2023): 1-20. <https://doi.org/10.1080/17455030.2023.2173504>
- [37] Nadeem, Sohail, Salman Akhtar, Nevzat Akkurt, Anber Saleem, Shahah Almutairi, and Hassan Ali Ghazwani. "Physiological peristaltic flow of Jeffrey fluid inside an elliptic cross section with heat and mass transfer: Exact solutions through Polynomial solution technique." *ZAMM-Journal of Applied Mathematics and Mechanics/Zeitschrift für Angewandte Mathematik und Mechanik* 103, no. 3 (2023): e202100383. <https://doi.org/10.1002/zamm.202100383>
- [38] Dyer, Raymond B., Michael YM Chen, and Ronald J. Zagoria. "Intravenous urography: technique and interpretation." *Radiographics* 21, no. 4 (2001): 799-824. <https://doi.org/10.1148/radiographics.21.4.g01j26799>
- [39] Wong, Siong Lung, and Hamzaini Abdul Hamid. "Observation of ureteric diameter in negative intravenous urogram in hospital Universiti Kebangsaan Malaysia." *The Malaysian journal of medical sciences: MJMS* 17, no. 2 (2010): 4.
- [40] Bradley, Desai, and Mamtora. "The relevance of parity to ureteric dilatation." *British journal of urology* 81, no. 5 (1998): 682-685. <https://doi.org/10.1046/j.1464-410x.1998.00641.x>
- [41] Itanyi, Ukamaka Dorothy, Joshua Oluwafemi Aiyekomogbon, Felix Uduma Uduma, and Matthew Abodunde Evinemi. "Assessment of ureteric diameter using contrast-enhanced helical abdominal computed tomography." *African Journal of Urology* 26 (2020): 1-5. <https://doi.org/10.1186/s12301-020-00021-0>
- [42] Hickling, Duane R., Tung-Tien Sun, and Xue-Ru Wu. "Anatomy and physiology of the urinary tract: relation to host

- defense and microbial infection." *Urinary tract infections: Molecular pathogenesis and clinical management* (2017): 1-25. <https://doi.org/10.1128/9781555817404.ch1>
- [43] Kohler, Tobias, Mitchell Yadven, Ankur Manvar, Nathan Liu, and Manoj Monga. "The length of the male urethra." *International braz j urol* 34 (2008): 451-456. <https://doi.org/10.1590/S1677-55382008000400007>
- [44] Keni, Laxmikant G., Mattias Jan Hayoz, Shah Mohammad Abdul Khader, Padmaraj Hegde, K. Prakashini, Masaaki Tamagawa, B. Satish Shenoy, BM Zeeshan Hameed, and Mohammad Zuber. "Computational flow analysis of a single peristaltic wave propagation in the ureter." *Computer Methods and Programs in Biomedicine* 210 (2021): 106378. <https://doi.org/10.1016/j.cmpb.2021.106378>
- [45] Bykova, A. A., and S. A. Regirer. "Mathematical models in urinary system mechanics." *Fluid Dynamics* 40, no. 1 (2005): 1-19. <https://doi.org/10.1007/s10697-005-0039-y>
- [46] Patankar, Suhas. *Numerical heat transfer and fluid flow*. Taylor & Francis, 2018. <https://doi.org/10.1201/9781482234213>
- [47] Jimenez Lozano JN. *Peristaltic Flow With Application To Ureteral*. PhD Thesis Mech Eng Notre Dame Univ Indiana, USA 2009:195.
- [48] Weinberg, S. L. "Ureteral function. I. Simultaneous monitoring of ureteral peristalsis." (1974).
- [49] Vahidi, Bahman, and Nasser Fatourae. "A numerical simulation of peristaltic motion in the ureter using fluid structure interactions." In *2007 29th Annual International Conference of the IEEE Engineering in Medicine and Biology Society*, pp. 1168-1171. IEEE, 2007. <https://doi.org/10.1109/IEMBS.2007.4352504>
- [50] Hosseini, G., C. Ji, D. Xu, M. A. Rezaenia, E. Avital, A. Munjiza, J. J. R. Williams, and J. S. A. Green. "A computational model of ureteral peristalsis and an investigation into ureteral reflux." *Biomedical Engineering Letters* 8 (2018): 117-125. <https://doi.org/10.1007/s13534-017-0053-0>